Influence of frequency on electrical and dielectric properties of $Au/Si_3N_4/n$-Si (MIS) structures

T. ATASEVEN, A. TATAROĞLU*, T. MEMMEDLI, S. ÖZÇELIK
Physics Department, Faculty of Sciences, Gazi University, 06500, Teknikokullar, Ankara, Turkey

In this study, we present a detailed investigation of the electrical and dielectric properties of the $Au/Si_3N_4/n$-Si (MIS) structures. The capacitance-voltage (C-V) and conductance-voltage (G/ω-V) characteristics have been measured in the frequency range of 1 kHz-1 MHz at room temperature. Calculation of the dielectric constant (ε'), dielectric loss (ε''), loss tangent (tanδ), ac conductivity (σ_{ac}) and complex electric modulus (M^*) are given in the studied frequency ranges. Experimental results show that the decrease of ε' and ε'' with the increasing frequency are observed. In addition, the increase of σ_{ac} with the increasing frequency is founded. Also, electric modulus formalism has been analyzed to obtain the experimental dielectric data. In addition, interfacial polarization can be more easily occurred at the lower frequency and/or with the number of interface state density between Si_3N_4/Si interface, consequently, contribute to the improvement of dielectric properties of MIS structure.

(Received May 18, 2012; accepted July 19, 2012)

Keywords: MIS structure; Electrical and dielectric properties; Ac conductivity; Electric modulus

1. Introduction

The metal-insulator-semiconductor (MIS) structures consist of semiconductor substrate that is covered by an insulator layer on which a metal electrode is deposited. Therefore, these structures constitute a kind of capacitor, which stores the electronic charges by virtue of dielectric property of insulator layers. The electrical characteristics of these structures are influenced by various non-idealities such as the interface states (N_{ss}), series resistance (R_s) and interfacial insulator layer [1-3]. Especially the performance and reliability of these structures are depending on the formation of insulator layer between metal and semiconductor interface and series resistance of devices. Also, the change in temperature has important effects on determination of structure parameters [4-6].

In general, there are several possible sources of error, which cause deviations from the ideal behavior. So, in calculations such as electrical and dielectric properties that includes the effects of interfacial insulator layer between metal and semiconductor; interface state density, series resistance and formation of barrier height must be taken into account. Nevertheless, satisfactory understanding in all details has still not been achieved.

Especially, the formation and characterization of insulator layers on substrate still remains a basic problem. It is well known that the high frequency electrical properties of MIS or metal-oxide-semiconductor (MOS) devices in the accumulation region describe basically the dielectric properties of the bulk oxide. Therefore, the real dielectric parameters of these devices were extracted from the strong accumulation capacitance and conductance. Thus, the effect of N_{ss} can be minimized at sufficiently high frequency C-V and G/ω-V measurements. At high frequencies ω (such the carrier life time τ is much larger than 1/ω) the charges at the interface states cannot follow an ac signal. In contrary, at low frequencies the charges can easily follow an ac signal and they are capable of increase with decreasing frequency. Therefore, the frequency dependent electrical and dielectric characteristics are very important according to accuracy and reliability of result [7-14].

Silicon nitride (Si_3N_4) is an industrially important material due to its chemical, mechanical, and electronic properties. Excellent thermomechanical properties have seen this material used for engine parts, bearings, metal machining, and other industrial applications. Silicon nitride is considered to be a promising material for microelectronic applications because of its high dielectric constant and large electronic gap [15,16].

In this study, we aimed to investigate the frequency effect on the electrical and dielectric properties of $Au/Si_3N_4/n$-Si (MIS) structure in the frequency range of 1 kHz-1 MHz at room temperature. To determining the dielectric constant (ε'), dielectric loss (ε''), loss tangent (tanδ), the ac conductivity (σ_{ac}) and complex electric modulus of MIS structure was used the admittance technique [8,12]. Also, it is well know, both electrical and dielectric properties of MIS structure significantly changes with frequency.

2. Experimental detail

$Au/Si_3N_4/n$-Si (MIS) structures were fabricated on a 2" diameter with (100) orientation, 300μm thickness, 0.5 Ω.cm resistivity and phosphorus doped (n-type) polycrystalline Si substrate. For the fabrication process,

the Si substrate was degreased in organic solvent of $CHClCCl_2$, CH_3COCH_3, and CH_3OH consecutively and then etched in a sequence of H_2SO_4 and H_2O_2 20% HF, a solution of $6HNO_3$:1HF:$35H_2O$, 20% HF and finally quenched in deionized water for a prolonged time. Preceding each cleaning step, the Si substrate was rinsed thoroughly in deionized water of resistivity of 18 MΩ.cm. Prior to film deposition, Si substrate was sputter cleaned in pure argon ambient after raising the substrate temperature to 400 ºC in $1x10^{-8}$ mbar high vacuum, to ensure the removal of any residual organics. Later, the Si substrate was transferred into the deposition chamber. Silicon nitride (Si_3N_4) thin film was deposited on n-Si using radio frequency (rf)-magnetron sputtering system and high purity (99.999%) silicon nitride target, under specific Ar+O_2 reactive gas mixture (Ar/O_2 = 90/10 sccm) controlled with mass flow controllers. For the deposition, the substrate temperature and the pressure was set to 200 ºC and $3x10^{-3}$ mbar, respectively and kept constant during the whole deposition.

The ohmic and rectifier contacts were formed using thermal evaporation system. The ohmic back contacts were formed by deposition of high purity Au (99.999%) with a thickness of ~2000 Å at 450 ºC, under 10^{-7} mbar vacuum and the sample was annealed at 400 ºC to achieve good ohmic contact behavior. After that, circular dot shaped rectifier front contacts with 1 mm diameter and ~2000 Å thickness were formed by deposition of high purity Au onto Si_3N_4 thin film at 50 ºC. In this way, Au/Si_3N_4/n-Si (MIS) structure was fabricated for the electrical measurements. The electrode connections were made by silver paste. The interfacial insulator layer thickness was estimated to be about 85 Å from measurement of the insulator capacitance in the strong accumulation region for MIS structure.

The capacitance-voltage (C-V) and conductance-voltage (G/ω-V) measurements were carried out in the frequency range of 1 kHz-1 MHz at room temperature, by using a HP 4192A LF impedance analyzer (5 Hz-13 MHz) and a small ac test signal 50 mV_{rms} from the external pulse generator was applied to the sample in order to meet the requirement. In addition, all measurements were carried out with the help of a microcomputer through an IEEE-488 ac/dc converter card.

3. Results and discussion

3.1. Frequency dependence of electrical properties

The conductance technique [2,3] is based on the conductance losses resulting from the exchange of majority carriers at the interface and majority carrier band of the semiconductor when a small ac signal is applied to the metal-insulator-semiconductor (MIS) structure. The applied ac signal causes the Fermi level to oscillate about the mean positions governed by the dc bias, when the MIS structure is in the depletion region.

Fig. 1(a) and (b) show the C-V and G/ω-V characteristics of the structure at various frequencies. It can be seen from Fig. 1(a) that at low frequencies, the values of capacitance are shown to increase. The frequency dependence of the capacitance can also arise due to the presence of deep lying impurities in the depletion region of semiconductor. Deep impurities are the energy levels of intrinsic lattice defects or impurity atoms that have energy near the center of the band gap. The higher values of capacitance at low frequencies are due to excess capacitance resulting from the interface states in equilibrium with the n-Si that can follow the ac signal. At high frequencies ω (such the carrier life time τ is much larger than 1/ω) the charges at the interface states cannot follow the ac signal. This makes the contribution of interface state capacitance to the total capacitance negligibly small [1,2,12,17-19].

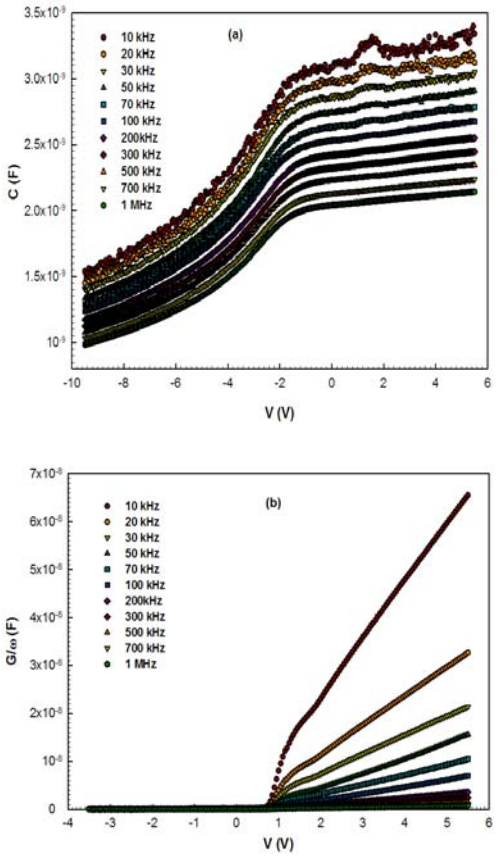

Fig. 1. The variation of the (a) C-V and (b) G/ω-V characteristics of Au/Si_3N_4/n-Si (MIS) structure measured for various frequencies at room temperature.

In addition, the variation of the C and G/ω with frequency at room temperature is shown in Figs. 2(a) and (b) of MIS structure, respectively. As shown in Figs. 2(a) and (b), the C and G/ω has displayed an increasing trend with the decreasing frequency. At low frequencies, the charges on neutral impurity defects are more readily redistributed, such that defects closer to the positive side of the applied field become negatively charged while the defects closer to the negative side of the field become positively charged. As the frequency is increased, the capacitance decreases to the same limit, as the charges on

the defects no longer have time to rearrange in response to the applied voltage [19-21].

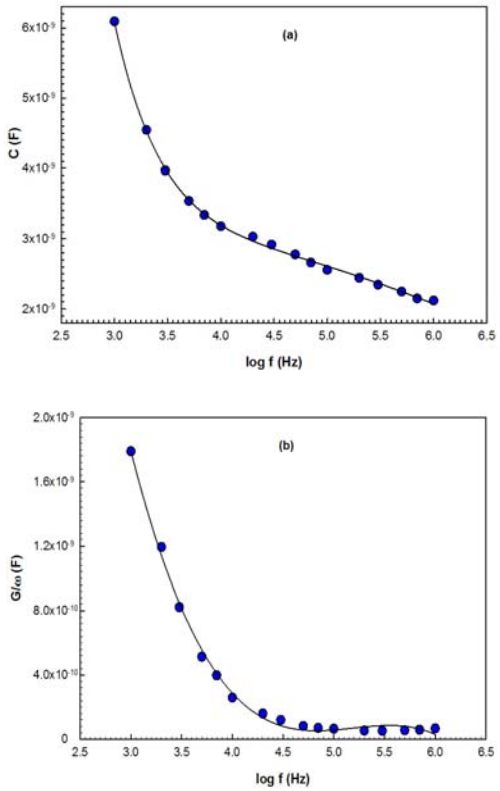

Fig. 2. The variation of (a) capacitance (C) and (b) conductance (G/ω) with log frequency of MIS structure at room temperature.

3.2. Frequency dependence of dielectric properties

The frequency dependence of dielectric constant (ε'), dielectric loss (ε''), loss tangent (tanδ), ac conductivity (σ_{ac}), and complex electric modulus (M^*) are studied for MIS structure. At room temperature, the values of the dielectric properties measured as a function of frequency in the 1 kHz to1 MHz range.

The complex permittivity can be defined in the following complex form [22,23],

$$\varepsilon^*(\omega) = \varepsilon'(\omega) - j\varepsilon''(\omega) \tag{1}$$

where ε' and ε'' are the real and the imaginary parts of complex permittivity, and j is the imaginary root of -1. The complex permittivity formalism has been employed to describe the electrical and dielectric properties. In the ε* formalism, in the case of admittance measurements, the following relation holds:

$$\varepsilon^* = \frac{Y^*}{j\omega C_o} = \frac{C}{C_o} - j\frac{G}{\omega C_o} \tag{2}$$

where Y^*, C and G are the measured admittance, capacitance and conductance of the dielectric and ω is the angular frequency (ω=2πf) of the applied electric field [24,25].

As it turns out the effect of conductivity can be highly suppressed when the data are presented in the modulus representation. The electric modulus approach began when the reciprocal complex permittivity was discussed as an electrical analogue to the mechanical shear modulus [26]. From the physical point of view, the electrical modulus corresponds to the relaxation of the electric field in the material when the electric displacement remains constant. Therefore, the modulus represents the real dielectric relaxation process [25-27]. The complex modulus $M^*(\omega)$ was introduced to describe the dielectric response of non-conducting materials. This formalism has been applied also to materials with non-zero conductivity. The starting point for further consideration is the definition of the dielectric modulus: [26,28].

$$M^*(\omega) = \frac{1}{\varepsilon^*} = M'(\omega) + jM''(\omega) \tag{3}$$

$$M'(\omega) = \frac{\varepsilon'(\omega)}{\varepsilon'(\omega)^2 + \varepsilon''(\omega)^2}$$

and

$$M''(\omega) = \frac{\varepsilon''(\omega)}{\varepsilon'(\omega)^2 + \varepsilon''(\omega)^2} \tag{4}$$

where M' and M'' are the real and the imaginary of complex modulus. Based on Eq. (4) we have changed the form of presentation of the dielectric data from $\varepsilon'(\omega)$ and $\varepsilon''(\omega)$ to $M'(\omega)$ and $M''(\omega)$.

The real part of the complex permittivity, the dielectric constant (ε'), at the various frequencies is calculated using the measured capacitance values at the strong accumulation region from the relation [9,13,22,25],

$$\varepsilon'(\omega) = \frac{C}{C_o} \tag{5}$$

where C_o is capacitance of an empty capacitor. $C_o = \varepsilon_o(A/d)$; where A is the rectifier contact area in cm^{-2}, d is the interfacial insulator layer thickness and ε_o is the permittivity of free space charge (ε_o = $8.85\text{x}10^{-14}$ F/cm). In the strong accumulation region, the maximal capacitance of MIS structure corresponds to the insulator capacitance (C_{ox}) ($C_{ac} = C_{ox} = \varepsilon'\varepsilon_o A/d$); where ε' is the dielectric constant of interfacial insulator layer (Si_3N_4) ($\varepsilon' = \varepsilon_i = 7.5\varepsilon_o$) [3].

The imaginary part of the complex permittivity, the dielectric loss (ε''), at the various frequencies is calculated using the measured conductance values from the relation,

$$\varepsilon''(\omega) = \frac{G}{\omega C_o} \tag{6}$$

The dissipation factor or loss tangent (tanδ) can be expressed as follows [22,23,25,29],

$$\tan\delta = \frac{\varepsilon''(\omega)}{\varepsilon'(\omega)} \tag{7}$$

The ac conductivity of all samples has been calculated from the dielectric losses according to the relation

$$\begin{aligned}\sigma^* &= j\varepsilon_o\omega\varepsilon^*(\omega) = j\varepsilon_o\omega(\varepsilon' - j\varepsilon'') \\ &= \varepsilon_o\omega\varepsilon'' + j\varepsilon_o\omega\varepsilon'\end{aligned} \tag{8}$$

The real part of $\sigma^*(\omega)$ is given by

$$\sigma_{ac} = \omega C \tan\delta(d/A) = \varepsilon_o\omega\varepsilon'' \tag{9}$$

The frequency dependencies of the ε', ε'' and tanδ of MIS structure are presented in Fig. 3(a), (b) and (c), respectively. As can be seen from these figures, ε' and ε'' decrease with an increase in frequency. This is the normal behavior of a dielectric material. In principle, at low frequencies and temperature, all the four types of polarization processes, i.e., the electronic, ionic, dipolar, and interfacial or surface polarization contribute to the values of ε' and ε''. With increasing frequency, the contributions of the interfacial, dipolar or the ionic polarization become ineffective by leaving behind only the electronic part. Furthermore, the decrease in ε' and ε'' with an increase in frequency is explained by the fact that as the frequency is raised, the interfacial dipoles have less time to orient themselves in the direction of the alternating field [30-36]. The ε' and ε'' have a values of 7.45, 2.19 at 1 kHz. This result shows that the strong low-frequency dispersion that characterizes the frequency dependence for the ε' and ε'' of MIS structure (in Fig 3(a) and (b)) has not been clearly understood. But in general, four possible mechanisms; electrode interface, ac conductivity, dipole-orientation and charge carriers may be contributed to be low-frequency dielectric behavior of MIS structure [31-34,37,38].

Especially, in the high frequency range, the values of ε' become closer to the values of ε''. This behavior of ε' and ε'' may be due to the interface states can not follow the ac signal at high frequency. Because the carrier lifetime of interface trapped charges (τ) are much larger than 1/ω at very high frequency (ω). Such this behavior was observed by several authors [9,13,39-42].

As shown in Fig. 3(c), the tanδ decreases with the increasing frequency. If the electric polarization in a dielectric is unable to follow the varying electric field, dielectric loss occurs. An applied field will alter this energy difference by producing a net polarization, which lags behind the applied field because the tunneling transition rates are finite. This part of the polarization, which is not in phase with the applied field, is termed as dielectric loss [43].

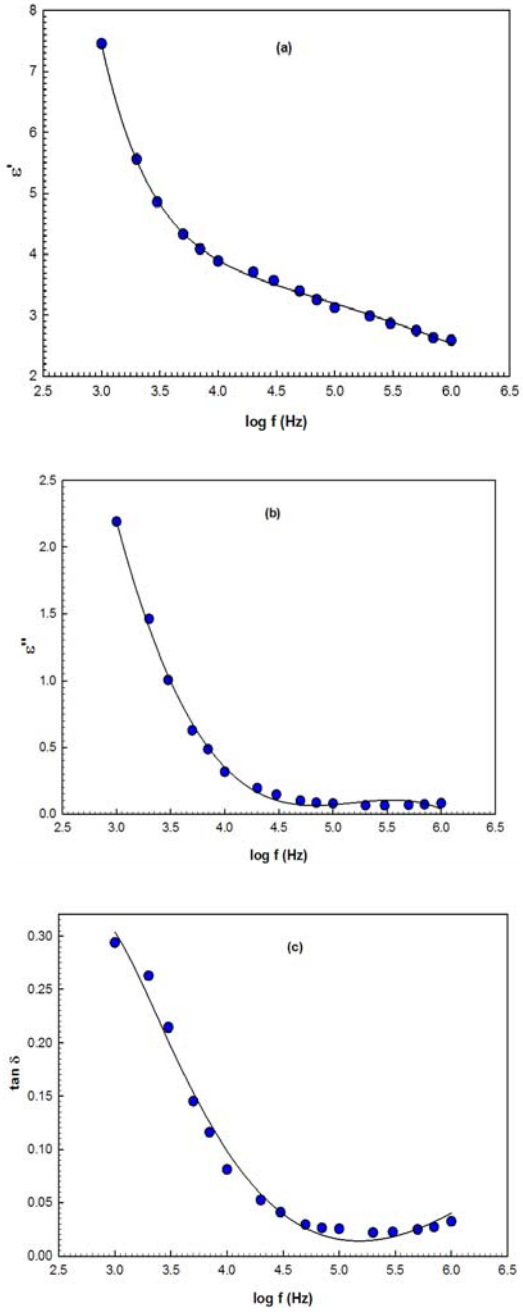

Fig. 3. Frequency dependence of the (a) ε', (b) ε'' and (c) tanδ at room temperature for MIS structure.

Fig. 4 illustrates the frequency dependence of ac conductivity (σ_{ac}) of MIS structure at room temperature. It is noticed that the σ_{ac} increases with the increasing frequency. This behaviour is typical for this structure and can be ascribed to the space charge polarization. As the frequency decreases, more and more charge accumulation occurs at the insulator-semiconductor interface, which leads to a drop in the conductivity at low frequencies [20,21,30-32,35,37,44-48].

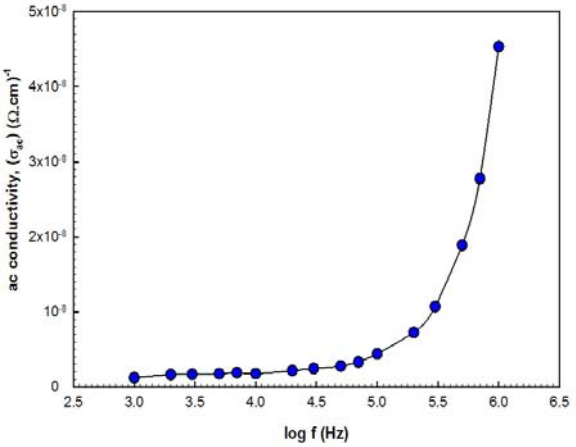

Fig. 4. Frequency dependence of ac conductivity (σ_{ac}) for MIS structure at room temperature.

The real component M' and imaginary component M'' were calculated from ε' and ε''. Fig. 5 shows the variation of the real (M') and imaginary part (M'') of complex modulus (M*) as a function of frequency at room temperature. As seen in Fig. 5 (a) and (b), the M' increases with the increasing frequency, while the M'' decreases with the increasing frequency. The imaginary part of complex modulus is indicative of energy loss in the structure under electrical field. Furthermore, the M'' gives a peak at about 2 kHz. The peak position suggests a frequency-dependent dielectric relaxation [21,30,37,49-51].

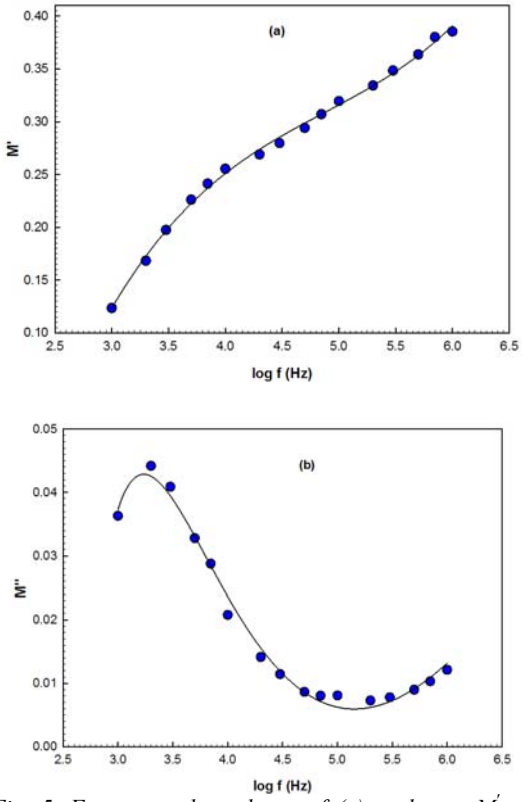

Fig. 5. Frequency dependence of (a) real part M' and (b) imaginary part M'' of complex electric modulus M at room temperature.*

4. Conclusions

This paper presents research pertaining to the frequency dependence of the electrical and dielectric properties of Au/Si_3N_4/n-Si (MIS) structure, which has been studied in detail in the frequency range of 1 kHz-1 MHz at room temperature. The values of capacitance and conductance decrease with the increasing frequency. This observation may be attributed to the capacitive response of interface states to the measurement. The values of the ε' and ε'' decrease with the increasing frequency. These behaviors are attributed to the decrease of polarization with increasing frequency in the Si_3N_4/n-Si interface. Also, the σ_{ac} increase with the increasing frequency due to the accumulation of charge carries at the boundaries. As a result, the behavior of electrical and dielectric properties especially depends on frequency, insulator layer, the density of space charges and interface states.

Acknowledgments

This work is supported by Gazi University Scientific Research Project (BAP), FEF. 05/2012-15.

References

[1] C.R. Crowell, S.M. Sze, J. Appl. Phys. **36**, 3212 (1965).
[2] E.H. Nicollian, J.R. Brews, Metal Oxide Semiconductor (MOS) Physics and Technology, Wiley, New York, 1982.
[3] S. M. Sze, Physics of Semiconductor Devices, 2nd Ed. Willey, New York 1981.
[4] Z Quennoughı, Phys. Stat. Sol.(a) **160**, 127 (1997).
[5] H.S. Haddara, M. El-Sayed, Solid State Electron. **31**, 1289 (1988).
[6] P.Cova, A. Singh, R.A. Masut, J. Appl. Phys. **82**, 5217 (1997).
[7] H. Deuling, E. Klausmann, A. Goetzberger, Solid State Electron. **15**, 559 (1972).
[8] S. Kar, S. Varma, J. Appl. Phys. **58**, 4256 (1985).
[9] A. Tataroğlu, Ş. Altındal, Microelectron. Eng. **85**, 1866 (2008).
[10] R. Castagne, A. Vapaille, Surface Sci. 28 (1971) 157.
[11] İ. Dökme, Ş. Altındal, M. Gökçen, Microelectron. Eng. **85**, 1910 (2008).
[12] E.H. Nicollian and A. Goetzberger, Appl. Phys. Let. **7**, 216 (1965).
[13] A. Tataroğlu, Ş. Altındal, M.M. Bülbül, Microelectron. Eng. **81**, 140 (2005).
[14] B. Akkal, Z. Benamara, B. Gruzza, L. Bideux, Vacuum **57**, 219 (2000).
[15] Y. Cai, L. Zhang, Q. Zeng, L. Cheng, Y. Xu, Phys. Review B **74**, 174301 (2006).
[16] F.L. Riley, J. Am. Ceram. Soc. **83**, 245 (2000).

[17] P. Chattopadhyay, B. Raychaudhuri, Solid State Electron. **35**, 605 (1993).
[18] Ş. Aydoğan, M. Sağlam, A. Türüt, Polymer **46**, 10982 (2005).
[19] J.H. Werner, Metallization and Metal-Semiconductor Interface, Plenum, New York, 1989.
[20] P. Matheswaran, R. Sathyamoorthy, R. Saravanakumar, S. Velumani, Mater. Sci. Eng. B **174**, 269 (2010).
[21] K. Prabakar, S.K. Narayandass, D. Mangalaraj, Phys. Stat. Sol. (a) **199**, 507 (2003)
[22] M. Popescu, I. Bunget, Physics of Solid Dielectrics, Elsevier, Amsterdam, 1984.
[23] A. Chelkowski, Dielectric Physics, Elsevier, Amsterdam, 1980.
[24] D. Cheng, Field and Wave Electromagnetics, 2nd Ed., Addison-Wesley, New York, 1989.
[25] P. Pissis, A. Kyritsis, Solid State Ionics **97**, 105 (1997).
[26] N.G. McCrum, B.E. Read and G. Williams, Anelastic and Dielectric Effects in Polymeric Solids, Wiley, New York, 1967.
[27] C. Leon, M.L. Lucia, J. Santamaria, Phys. Rev. B **55**, 882 (1998).
[28] F. Yakuphanoğlu, I.S. Yahia, B.F. Senkald, G.B. Sakrc, W.A. Farooq, Synthetic Metals **161**, 817 (2011).
[29] C.P. Symth, Dielectric Behaviour and Structure, McGraw-Hill, New York, 1955.
[30] S.P. Szu, C.Y. Lin, Mater. Chem. Phys. **82**, 295 (2003).
[31] D. Maurya, J. Kumar, Shripal, J. Phys. Chem. Solids **66**, 1614 (2005).
[32] D.R. Patil, B.K. Chougule, J. Alloys Comp. **470**, 531 (2009).
[33] S. Maity, D. Bhattacharya, S.K. Ray, J. Phys. D: Appl. Phys. **44**, 095403 (2011).
[34] A. Tataroğlu, J. Optoelectron. Adv. Mater. **13**, 940 (2011).
[35] J.S. Kim, H.J. Lee, S.Y. Lee, I.W. Kim, S.D. Lee, Thin Solid Films **518**, 6390 (2010).
[36] A. Eroğlu, A. Tataroğlu, Ş. Altındal, Microelectron. Eng. **91**, 154 (2012).
[37] I.S. Yahia, M.S. Abd El-sadek, F. Yakuphanoğlu, Dyes and Pigments **93**, 1434 (2012).
[38] T. Tunç, İ. Uslu, İ. Dökme, Ş. Altındal, H. Uslu, I. J. Poly. Mater. **59**, 739 (2010).
[39] A.K. Dubey, P. Singh, S. Singh, D. Kumar, O. Parkash, J. Alloys Compd. **509**, 3899 (2011).
[40] C. V. Kannan, S. Ganesamoorthy, C. Subramanian, P. Ramasamy, Phys. Stat. Sol. (a) **196**, 465 (2003).
[41] Z. Jiwei, Y. Xi, W. Mingzhong, Z. Liangying, J. Phys. D: Appl. Phys. **34**, 1413 (2001).
[42] L. Kungumadevi, R. Sathyamoorthy, A. Subbarayan, Solid State Electron. **54**, 58 (2010).
[43] M. Rapos, M. Ruzinsky, S. Luby, J. Cervenk, Thin Solid Films **36**, 103 (1976).
[44] A.S. Riad, M.T. Korayem, T.G. Abdel-Malik, Physica B **270**, 140 (1999).
[45] M.M. Abdel Kader, M.Y. Elzayat, T.R. Hammad, A.I. Aboud, H. Abdelmonem, Phys. Scr. **83**, 035705 (2011).
[46] K.C. Verma, M. Ram, J. Singh, R.K. Kotnala, J. Alloys Compd. **509**, 4967 (2011).
[47] S.C. Watawe, B.D. Sarwade, S.S. Bellad, B.D. Sutar, B.K. Chougule, J. Magnetism Magnetic Materials **214**, 55 (2000).
[48] B. Taraev, Physics of Dielectric Materials, Mir Publication, Moscow, 1975.
[49] F. Yakuphanoğlu, Physica B **393**, 139 (2007).
[50] N. Singh, A. Agarwal, S. Sanghi, Current Appl. Phys. **11**, 783 (2011).
[51] M.B. Mohamed, H. Wang, H. Fuess, J. Phys. D: Appl. Phys. **43**, 455409 (2010).

*Corresponding author: ademt@gazi.edu.tr